

Study of the upper bound of tool edge radius in nanoscale ductile mode cutting of silicon wafer

Xiaoping Li · Minbo Cai · M. Rahman · Steven Liang

Received: 6 January 2008 / Accepted: 28 September 2009 / Published online: 10 November 2009
© Springer-Verlag London Limited 2009

Abstract In cutting of brittle materials, experimentally it was observed that there is an upper bound of tool cutting edge radius, beyond which, although the undeformed chip thickness is smaller than the tool cutting edge radius, the ductile mode cutting cannot be achieved. However, why there is an upper bound of tool cutting edge radius in nanoscale ductile mode cutting of brittle materials has not been fully understood. In this study, based on the tensile stress distribution and the characteristics of the distribution obtained from molecular dynamics simulation of nanoscale ductile cutting of silicon, an approximation for the tensile stress distribution was obtained. Using this tensile stress distribution with the principles of geometrical similarity and fracture mechanics, the critical conditions for the crack initiation have been determined. The result showed that there is a critical tool cutting edge radius, beyond which crack initiation can occur in the nanoscale cutting of silicon, and the chip formation mode is transferred from ductile to brittle. That is, this critical tool cutting edge radius is the upper bound of the tool cutting edge radius for ductile mode cutting of silicon.

X. Li (✉) · M. Cai · M. Rahman
Department of Mechanical Engineering,
National University of Singapore,
Singapore 119260, Singapore
e-mail: mpelixp@nus.edu.sg

M. Cai
e-mail: caiminbo@nus.edu.sg

M. Rahman
e-mail: mpemusta@nus.edu.sg

S. Liang
George W. Woodruff School of Mechanical Engineering,
Georgia Institute of Technology,
Atlanta, GA 30332, USA
e-mail: steven.liang@me.gatech.edu

Keywords Nanoscale cutting · Silicon wafer · Molecular dynamics · Upper bound · Crack initiation

1 Introduction

Many researchers have reported the results for nanoscale ductile cutting of brittle materials, such as silicon and germanium [1–5]. It has been well recognized that ductile machining of monocrystalline silicon can be achieved when undeformed chip thickness is down to several tens of nanometers. Liu and Li [6] further observed only that when the undeformed chip thickness is smaller than the tool cutting edge radius of the zero rake angle (the tool cutting edge radius R and the undeformed chip thickness a_c are shown in Fig. 1), the ductile mode cutting can be achieved. In practical application, for high production rate, the undeformed chip thickness and the tool cutting edge radius are both expected to be as large as possible when the undeformed chip thickness is smaller than the tool cutting edge radius. However, Arefin et al. [7] found that there is an upper bound value for the tool cutting edge radius, above which the chip formation mode changes from ductile to brittle even though the undeformed chip thickness remains to be smaller than the tool edge radius.

Some researchers have attempted to explain why there is a critical threshold of the undeformed chip thickness in the ductile mode cutting of brittle materials. One of the explanations is based on a model [8] for crack initiation in elastic/plastic indentation fields. In this model, Lawn and Evans obtained a lower bound of the critical crack length C^* and the critical load P^* to the requirements for crack initiation in the indentation,

$$C^* = \alpha(K_c/H)^2, P^* = \beta(K_{lc}/H)^3 K_{lc} \quad (1)$$

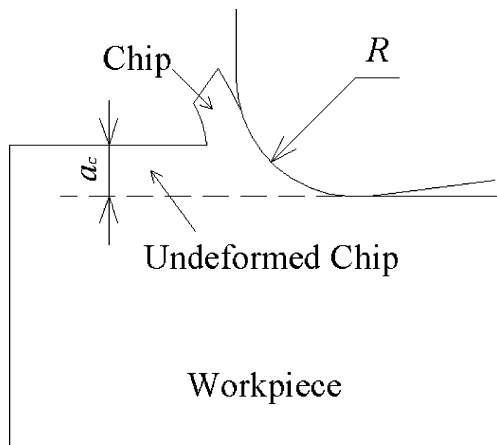


Fig. 1 The schematic of cutting process

where α and β are constants for different materials, K_{Ic} is the critical stress intensity factor, and H is the material hardness. Below this critical load P^* , no crack will be initiated. Corresponding to this critical condition, Marshall and Lawn [9] proposed that the critical indent size t^* is scaled to the critical crack length C^* ,

$$t^* = \mu(K_{Ic}/H)^2 \quad (2)$$

where $\mu \propto E/H$, and E is the elastic modulus. Based on Eq. 2, Blake and Scattergood [1] and Blackley and Scattergood [10] claimed that although the chip formation action of a diamond turning tool differs dynamically and geometrically from the deformation produced using indentation, there are essential similarities in both processes, and it will be hypothesized that a critical depth parameter t^* will divide fracture from ductility in ultraprecision. They also developed a model for single-point diamond turning of brittle materials to determine the critical depth parameter in a certain machining condition by experiments [1, 10]. Puttick et al. [11] used a critical linear dimension d_c of the stressed volume of material to predict the critical depth of cut in the machining of glass,

$$d_c = \alpha E R_c / \sigma_y^2 \quad (3)$$

where σ_y is the yield stress for plastic flow, and R_c is the specific work per unit area required to propagate a crack.

Although these researches have been done to study the critical undeformed chip thickness in micro/nanoscale cutting of brittle materials, they ignored a very important parameter, the tool cutting edge radius, and assumed that the tools were sharp. In nanoscale cutting of materials, where the undeformed chip thickness can be well below 100 nm and the smallest cutting edge radius of a single crystal diamond tool may still be in the range of 20–70 nm, this assumption is obviously not reasonable. Moreover, their analysis was mostly based on the indentation, and the

indenter was supposed to be sharp. In the indentation, the workpiece material is compressed and will not be removed, but in the cutting the workpiece material is removed and the chip forms.

So, the different material deformation and tool shape would lead to different stress distribution in the machining zone and consequently different transition mechanism from ductile to brittle mode chip formation when the cutting scale size changes.

In this study, the phenomenon that there is an upper bound of tool edge radius in nanoscale ductile mode cutting of silicon wafer has been explained. The molecular dynamics (MD) method was used to simulate the nanoscale ductile mode cutting of monocrystalline silicon. The MD simulation result of stress showed that the tensile stress exists in a small area, which borders up the interface of plastic and elastic deformation zones, and the location of the maximum tensile stress is near to this interface. Based on the tensile stress distribution and the characteristics of the distribution obtained from MD simulation, a simple approximation for the tensile stress distribution was given. Using this tensile stress distribution with the principles of geometrical similarity and fracture mechanics, the critical conditions for the crack initiation have been determined. The analysis showed that there is a critical tool cutting edge radius beyond which crack initiation can occur in the nanoscale cutting of silicon, and the chip formation mode is transferred from ductile to brittle. Therefore, this critical tool cutting edge radius is the upper bound of the tool cutting edge radius for the ductile mode cutting of silicon.

2 The tensile stress distribution and the cutting force

To study the stress distribution in the workpiece and cutting force during cutting, the molecular dynamics method has been used to model and simulate the nanoscale cutting of silicon. Nanoscale cutting involves workpiece deformation in only a few atomic layers near the workpiece surface. At such a small governing length scale, the continuum representation of the problem becomes questionable. To study such a process, the molecular dynamics simulation method seems to be more appropriate. The basic MD method and simulation model have been described in Ref. [12]. In this MD simulation, a three-dimensional model has been developed for the nanoscale ductile mode cutting of silicon, as shown in Fig. 2, where (a) shows a schematic diagram of the MD model and (b) shows an output of the MD simulation system. The x direction is the cutting direction.

A series of simulations have been carried out under different cutting edge radii, which are 2.5, 4.0, and 6.0 nm, respectively. In the simulations, the ratio of undeformed

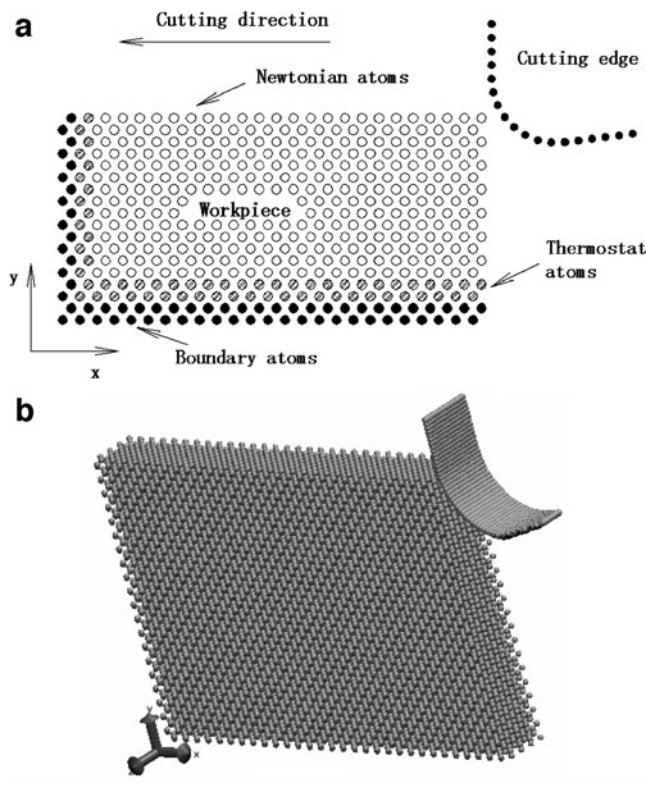


Fig. 2 The model for the MD simulation of nanoscale cutting: **a** a schematic of the MD model and **b** a model output from the MD simulation system

chip thickness to the cutting edge radius is fixed at 0.8, so that the corresponding undeformed chip thicknesses are 2, 3.2, and 4.8 nm, respectively. This cutting condition ensures that the chip formation is in ductile mode. The working environment temperature is set at 293 K and the cutting speed is set at 20 m/s.

Figure 3 shows a snapshot of the MD simulation of nanoscale cutting process. The normal stress along the y

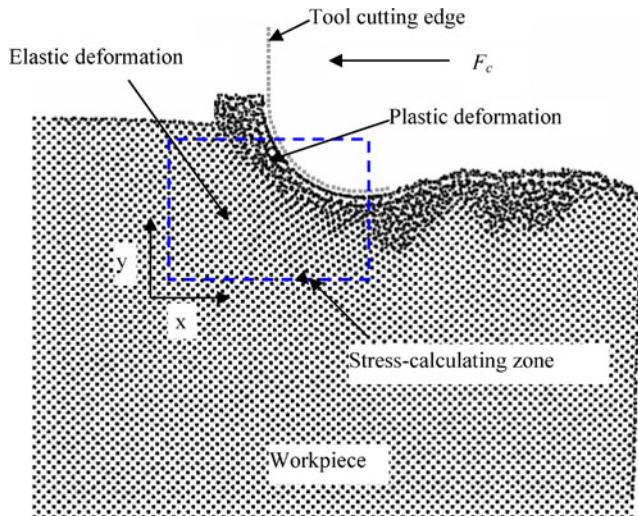


Fig. 3 A snapshot of the MD simulation of nanoscale cutting process

direction σ_{yy} in the stress-calculating zone as shown in Fig. 3 has been calculated. Figures 4, 5, and 6 show the normal stress σ_{yy} distributions in the stress-calculating zone under different cutting conditions, $R=2.5$ nm and $a_c=2.0$ nm, $R=4.0$ nm and $a_c=3.2$ nm, and $R=6.0$ nm and $a_c=4.8$ nm, respectively. From these figures, it can be seen that in most areas of the stress-calculating zone, σ_{yy} is compressive stress and only in a small area is its tensile stress (the positive value represents compressive stress and the negative value tensile stress). It also can be seen that this small area with tensile stress borders upon the interface of plastic and elastic deformation zones as shown in Fig. 3. Moreover, the maximum value of tensile stress σ_{yy} will increase, and the location of the maximum tensile stress σ_{yy} will be nearer to the interface of plastic and elastic deformation zones.

Based on this tensile stress distribution and the characteristics of the distribution obtained from MD simulation of nanoscale cutting of silicon, a simple linear approximation for the tensile stress distribution is given as shown in Fig. 7 when the tool cutting edge radius reaches its upper bound,

$$\sigma(x) = \begin{cases} \sigma_m(1 - x/b) & (x \leq b) \\ 0 & (x \geq b) \end{cases}. \quad (4)$$

where b is the size of tensile stress field, and σ_m represents the maximum tension at the interface. The actual tensile stress field is extremely complex and should depend on other parameters. Moreover, out of the range b , the normal stress in y direction is compressive stress. However, this simplified linear stress distribution is essentially same as the complex stress field [13], and it will be useful to deduce the formulation.

The cutting force F_c (see Fig. 3) acting on the cutting tool in the cutting direction at the different tool cutting edge radius is shown in Fig. 8, which indicates that when the tool

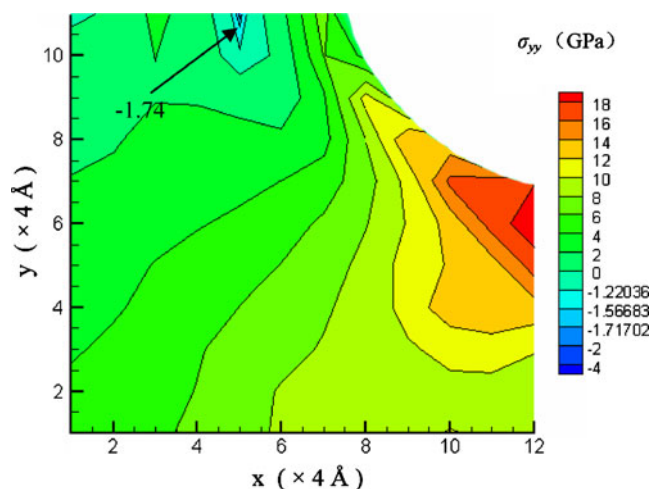


Fig. 4 The normal stress σ_{yy} distribution in the stress-calculating zone when $R=2.5$ nm and $a_c=2.0$ nm

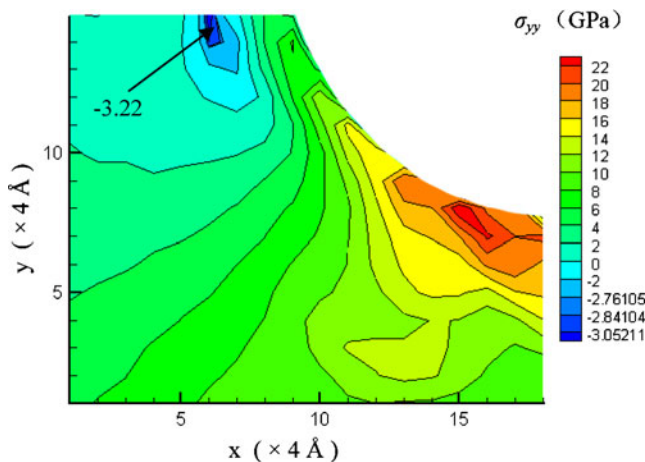


Fig. 5 The normal stress σ_{yy} distribution in the stress-calculating zone when $R=4.0$ nm and $a_c=3.2$ nm

cutting edge radius increases, the cutting force acting on the cutting tool also increases.

3 A model for crack initiation in nanoscale cutting

3.1 Defect

In the plastic deformation zone (the size d as shown in Fig. 7), there is a phase transformation of the monocrystalline silicon from diamond cubic structure to both β silicon and amorphous phase due to the high compressive stress [14]. Therefore, the interface of plastic and elastic deformations is similar to a grain boundary. Because of the different lattice structures in the plastic and elastic deformation zones, the small defect will occur at the interface, which has been shown in Fig. 7 with the length c .

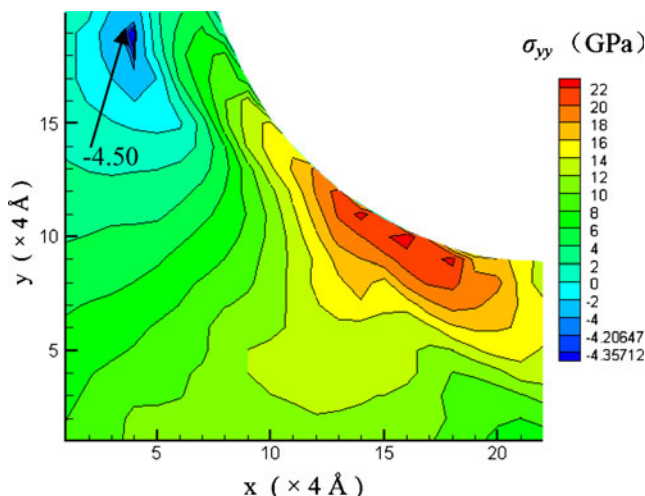


Fig. 6 The normal stress σ_{yy} distribution in the stress-calculating zone when $R=6.0$ nm and $a_c=4.8$ nm

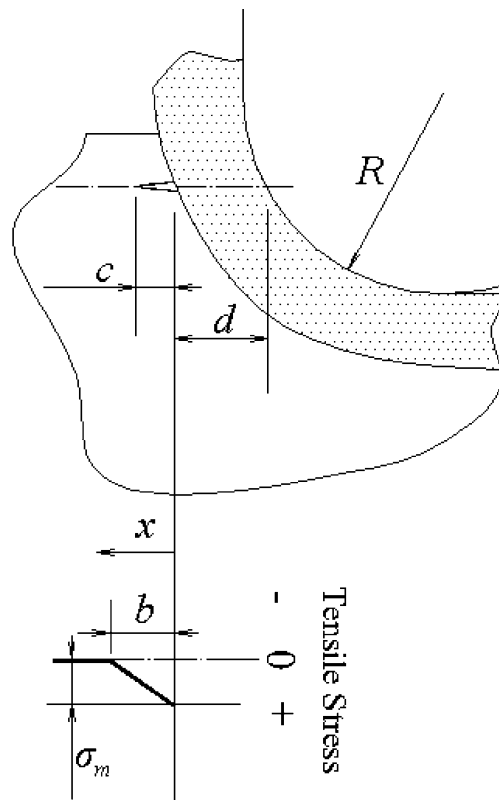


Fig. 7 The model for the edge crack initiation in nanoscale cutting of silicon

3.2 Model for crack initiation

As shown in Fig. 7, a model for crack initiation has been proposed. In the tensile stress area, there is a defect at the interface of plastic and elastic deformation zones. With this tensile stress, the defect is possible to propagate and form

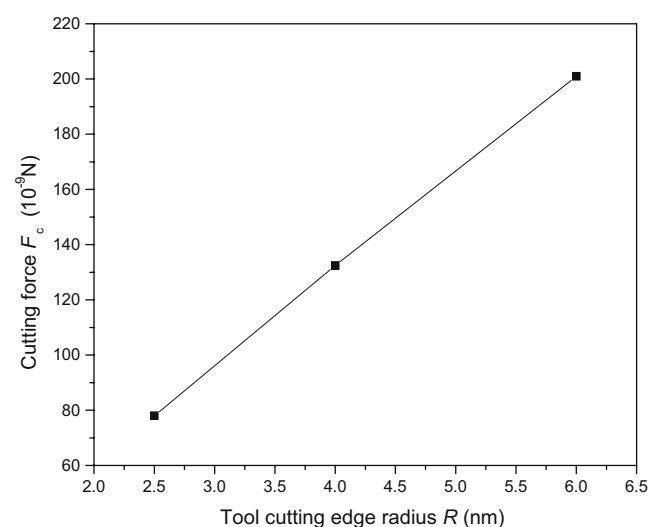


Fig. 8 The cutting force F_c acting on the cutting tool at the different tool cutting edge radius

an edge crack, but when the tensile stress is not enough for the defect propagation, the defect will be stable, so the crack will not be initiated, and chip is formed in ductile mode. Since the tensile stress will increase when the tool cutting edge radius increases as mentioned in Section 2, there should be an upper bound of the tool cutting edge radius for the ductile mode chip formation.

In order to determine the critical condition of defect propagation, the stress intensity factor for this edge crack in the tensile stress field should be evaluated. The Green function for an edge crack loaded by a pair of force P is [15]

$$K_I = \frac{2}{3} \frac{P}{\sqrt{\pi c}} \frac{4 - \left(\frac{x}{c}\right)}{\sqrt{1 - \left(\frac{x}{c}\right)^2}}, \quad (5)$$

$$K_I = (\sigma_m/3)(c/\pi)^{1/2} \left\{ (8c/b + 1)(1 - b^2/c^2)^{1/2} + (8 + c/b) \tan^{-1} \left[1/(c^2/b^2 - 1)^{1/2} \right] - 8c/b - 2 \right\}, \quad c \geq b. \quad (7b)$$

The MD simulation result has shown that when the tool cutting edge radius increases, the cutting force acting on the cutting tool also increases. So, when the tool cutting edge radius just reaches the critical value for crack initiation, the cutting force F_c in the cutting direction also reaches the maximum value F_m . A new material hardness, the cutting hardness H_c , is defined using the maximum value F_m ,

$$H_c = F_m / (\lambda_1 W_h W_w), \quad (8)$$

where λ_1 is a dimensionless factor determined by the tool geometry, W_h is the height of the area subject to cutting force in the cutting direction, and W_w is the width of the area subject to cutting force. Both W_h and W_w are scaled with the tool cutting edge radius R using coefficients λ_2 and λ_3 , respectively,

$$W_h = \lambda_2 R, \quad W_w = \lambda_3 R. \quad (9)$$

H_c represents the resistance ability to crack initiation, which is similar to the indentation hardness H or scratching

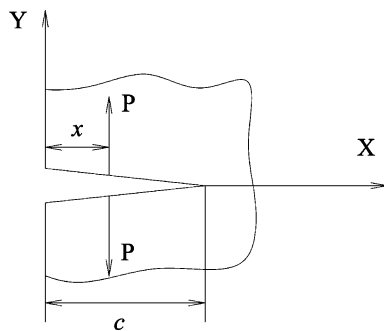


Fig. 9 An edge crack

where K_I is the stress intensity factor, c is the initial length of the crack, and x represents the place of the force P as shown in Fig. 9. Based on this green function, use the Schwartz alternating method to develop a first approximation for the stress intensity factor for this edge crack in the simplified linear stress field,

$$K_I = \frac{2}{3} \frac{1}{\sqrt{\pi c}} \int_0^c \sigma(x) dx \frac{4 - \left(\frac{x}{c}\right)}{\sqrt{1 - \left(\frac{x}{c}\right)^2}}. \quad (6)$$

Substitute Eq. 4 into Eq. 6, and the stress intensity factors are obtained in different conditions,

$$K_I = (2\sigma_m/3)(c/\pi)^{1/2} [2\pi - 1 + (\pi/4 - 4)(c/b)], \quad c \leq b, \quad (7a)$$

hardness H_s of brittle materials and should be a constant of the material property. It is supposed that for monocrystalline silicon the ratio of the cutting hardness to the indentation hardness is ζ [16],

$$H_c = \zeta H. \quad (10)$$

The maximum tensile stress should scale directly with the cutting hardness in the cutting direction [8], that is

$$\sigma_m = \theta H_c = \theta \zeta H, \quad (11)$$

where θ is a dimensionless factor. The size of tensile stress field b also should scale with the tool size R , so

$$b = \eta R = \eta [F_m / (\zeta \lambda_1 \lambda_2 \lambda_3 H)]^{1/2}, \quad (12)$$

where η is another dimensionless constant. According to the Griffith criterion, when the crack start to grow, K_I should reach the critical stress intensity factor K_{Ic} , that is,

$$K_I = K_{Ic}. \quad (13)$$

Substitute Eqs. 11, 12, and 13 into Eqs. 7a and 7b, and after simplification, the critical condition equations for the crack growth can be obtained as in the following:

$$1 = 2C^{1/2} [2\pi - 1 + (\pi/4 - 4)(C/F^{1/2})], \quad C^2 \leq F, \quad (14a)$$

$$1 = C^{1/2} \left\{ \left(8C/F^{1/2} + 1 \right) (1 - F/C^2)^{1/2} + (8 + C/F^{1/2}) \tan^{-1} \left[1/(C^2/F - 1)^{1/2} \right] - 8C/F^{1/2} - 2 \right\}, \quad C^2 \geq F, \quad (14b)$$

where C and F are the nominal defect length and nominal cutting force, respectively,

$$C = [(\theta\zeta H)/(3\pi^{1/2}K_{lc})]^2 c, \quad (15a)$$

$$F = [(\eta^2\theta^4\zeta^3H^3)/(81\pi^2\lambda_1\lambda_2\lambda_3K_{lc}^4)]F_m. \quad (15b)$$

3.3 Discussion

Equations 14a and 14b only have two variables, and it is can be set that F is the function of variable C . Based on this, the solution of function $F(C)$ can be plotted as shown in Fig. 10. Since Eqs. 14a and 14b represent the critical condition for the crack growth, the curve of function $F(C)$ shows the critical nominal cutting force F corresponding to the different nominal defect length C when the crack begins to grow. From Fig. 10, it can be seen that there is a lowest point ($C^*=0.02015$, $F^*=0.00135$) along the curve of $F(C)$, where

$$C^* = 0.02015, \quad (16a)$$

$$F^* = 0.00135, \quad (16b)$$

that is, when the nominal cutting force is smaller than F^* , the defect will not extend regardless of the size and place of defect. Therefore, the lowest point is a critical point, and only when the nominal defect length and nominal cutting

force both reach the critical value C^* and F^* , respectively, the crack is possible to propagate.

According to Eqs. 15a and 15b and 16a and 16b, the critical defect length and critical cutting force for the crack initiation can be obtained as in the following:

$$c^* = [0.5697/(\theta^2\zeta^2)](K_{lc}/H)^2, \quad (17a)$$

$$F_m^* = [(1.079\lambda_1\lambda_2\lambda_3)/\eta^2\theta^4\zeta^3]K_{lc}^4/H^3. \quad (17b)$$

Based on the assumption that the defect length for the crack initiation scales directly with the machining size [9], which is the tool cutting edge radius R here, the critical tool cutting edge radius R^* can be obtained,

$$R^* = \kappa c^* = [0.5697\kappa/(\theta^2\zeta^2)](K_{lc}/H)^2, \quad (18)$$

where κ is a dimensionless factor and represents the ratio of the critical tool cutting edge radius to the critical defect length. Since the tool cutting edge radius is beyond the critical value R^* , the crack initiation becomes possible, and the chip formation mode will be transferred from the ductile to brittle, the critical tool cutting edge radius R^* is the upper bound of tool edge radius in nanoscale ductile mode cutting of silicon wafer. Equation 18 indicates that the upper bound of the tool cutting edge radius mainly depends on the ratio of the critical stress intensity factor to the indentation hardness of the material, and this is same as the result of indentation (see Eq. 2).

4 Conclusions

In this study, the phenomenon that there is an upper bound of tool edge radius in nanoscale ductile mode cutting of silicon wafer has been explained. The MD method was used to simulate the nanoscale ductile mode cutting of monocrystalline silicon. The MD simulation result of stress showed that the tensile stress exists in a small area, which borders up the interface of plastic and elastic deformation zones, and the location of the maximum tensile stress is near to this interface. Based on the tensile stress distribution and the characteristics of the distribution obtained from MD simulation, a simple approximation for the tensile stress distribution was obtained. Using this tensile stress distribution with the principles of geometrical similarity and fracture mechanics, the critical conditions for the crack initiation has been determined. The analysis showed that

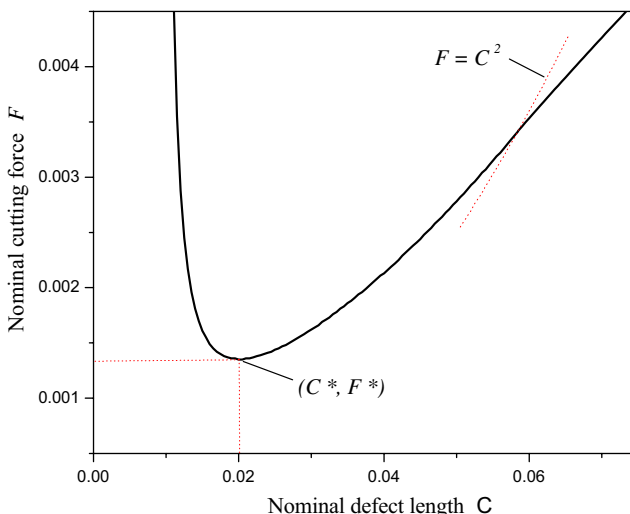


Fig. 10 Plot of function $F(C)$

there is a critical tool cutting edge radius beyond which crack initiation can occur in the nanoscale cutting of silicon, and the chip formation mode is transferred from ductile to brittle. Therefore, this critical tool cutting edge radius is the upper bound of the tool cutting edge radius for the ductile mode cutting of silicon.

References

1. Blake PN, Scattergood RO (1990) Ductile-regime machining of germanium and silicon. *J Am Ceram Soc* 73(4):949–957
2. Puttick KE, Whitmore LC, Zhdan P, Gee AE, Chao CL (1995) Energy scaling transitions in machining of silicon by diamond. *Tribol Int* 28(6):349–355
3. Fang FZ, Venkatesh VC (1998) Diamond cutting of silicon with nanometric finish. *CIRP Ann* 47(1):45–49
4. Leung TP, Lee WB, Lu XM (1998) Diamond turning of silicon substrates in ductile-regime. *J Mater Process Technol* 73:42–48
5. Yan J, Yoshino M, Kuriyagawa T, Shirakashi T, Syoji K, Komanduri R (2001) On the ductile machining of silicon for micro electro-mechanical systems (MEMS), opto-electronic and optical applications. *Mater Sci Eng A* 297(1/2):230–234
6. Liu K, Li XP (2001) Modeling of ductile cutting of tungsten carbide. *Transactions of NAMRI/SME XXIX*:251–258
7. Arefin S, Li XP, Rahman M, Liu K (2007) The upper bound of tool edge radius for nanoscale ductile mode cutting of silicon wafer. *Int J Adv Manuf Technol* 31:655–662
8. Lawn BR, Evans AG (1977) A model for crack initiation in elastic/plastic indentation fields. *J Mater Sci* 12:2195–2199
9. Marshall DB, Lawn BR (1986) Indentation of brittle materials. In: *Microindentation Technology in Materials Science and Engineering, ASTM STP 889*:26–46
10. Blackley WS, Scattergood RO (1991) Ductile-regime machining model for diamond turning of brittle materials. *Precis Eng* 13(2):95–103
11. Puttick KE, Rudman MR, Smith KJ, Franks A, Klindsey K (1989) Single-point diamond machining of glasses. *Proc R Soc Lond A* 426:19–30
12. Cai MB, Li XP, Rahman M (2007) Molecular dynamics modeling and simulation of nanoscale ductile cutting of silicon. *Int J Comput Appl Technol* 28(1):2–8
13. Lawn BR, Evans AG (1977) A model for crack initiation in elastic/plastic indentation fields. *J Mater Sci* 12:2195–2199
14. Cai MB, Li XP, Rahman M (2007) High-pressure phase transformation as the mechanism of ductile chip formation in nanoscale cutting of silicon wafer. *Proc IMechE Part B: J. Engineering Manufacture* 221:1511–1519
15. Tada H, Paris PC, Irwin GR (2000) The stress analysis of cracks handbook. ASME, New York, p 71
16. Ichimura H, Rodrigo A (2000) The correlation of scratch adhesion with composite hardness for TiN coatings. *Surf Coat Technol* 126:152–158